THE JOURNAL OF BIOLOGICAL CHEMISTRY
Vol. 279, No. 45, Issue of November 5, pp. 47192–47200, 2004

Structural Basis for the Inhibitory Role of Tomosyn in Exocytosis*[S] ♦

Received for publication, August 2, 2004, and in revised form, August 10, 2004
Published, JBC Papers in Press, August 16, 2004, DOI 10.1074/jbc.M408767200

Ajaybabu V. Pobbati‡, Adelia Razeto§¶, Matthias Böddener‡, Stefan Becker§, and Dirk Fasshauer‡‖

From the ‡Department of Neurobiology, §Department of NMR-based Structural Biology, Max-Planck-Institute for Biophysical Chemistry, Am Fassberg 11, 37077 Göttingen, Germany

Upon Ca^{2+} influx synaptic vesicles fuse with the plasma membrane and release their neurotransmitter cargo into the synaptic cleft. Key players during this process are the Q-SNAREs syntaxin 1a and SNAP-25 and the R-SNARE synaptobrevin 2. It is thought that these membrane proteins gradually assemble into a tight trans-SNARE complex between vesicular and plasma membrane, ultimately leading to membrane fusion. Tomosyn is a soluble protein of 130 kDa that contains a COOH-terminal R-SNARE motif but lacks a transmembrane anchor. Its R-SNARE motif forms a stable core SNARE complex with syntaxin 1a and SNAP-25. Here we present the crystal structure of this core tomosyn SNARE complex at 2.0-Å resolution. It consists of a four-helical bundle very similar to that of the SNARE complex containing synaptobrevin. Most differences are found on the surface, where they prevented tight binding of complexin. Both complexes form with similar rates as assessed by CD spectroscopy. In addition, synaptobrevin cannot displace the tomosyn helix from the tight complex and vice versa, indicating that both SNARE complexes represent end products. Moreover, data bank searches revealed that the R-SNARE motif of tomosyn is highly conserved throughout all eukaryotic kingdoms. This suggests that the formation of a tight SNARE complex is important for the function of tomosyn.

Synaptic exocytosis is a highly controlled form of vesicular trafficking evolved to rapidly release neurotransmitter into the synaptic cleft. Neurotransmitter-loaded synaptic vesicles reside in a ready-to-fuse state close to the plasma membrane. Upon the influx of Ca^{2+} they undergo rapid fusion. Many protein components of the release machinery have been identified, but their exact roles are only gradually coming to light. Several factors of the synaptic release machinery are common to all fusion events of the secretory pathway. Among them the SNARE[1] proteins are thought to play a catalytic role in the membrane fusion process. Best characterized are the SNARE proteins involved in synaptic exocytosis. They include the synaptic vesicle protein synaptobrevin 2 (also referred to as vesicle-associated membrane protein 2 (VAMP 2)) and the plasma membrane proteins syntaxin 1a and SNAP-25, which form a tight ternary complex between the two membranes. SNARE monomers are mostly unstructured but upon assembly into the ternary complex major conformational changes occur (1, 2). The crystal structure of the core region of the ternary SNARE complex revealed that the complex consists of an elongated, parallel four-helix bundle (3). Consequently, during assembly of the ternary complex, the transmembrane regions of the SNAREs, which are originally located in opposing membranes, end up on the same side of the complex. Therefore, as a general principle, it is thought that SNARE assembly brings the opposing membranes into close apposition, perhaps directly causing membrane fusion (for reviews, see Refs. 4–8).

The SNARE four-helix bundle contains one helix each of synaptobrevin 2 and syntaxin 1a, whereas SNAP-25 contributes two helices. Over the length of the coiled-coil bundle, 16 heptad repeat layers are formed that are mostly hydrophobic. In the center, however, a buried hydrophilic heptad repeat layer ("0-layer") exists. It consists of three glutamine residues (Q), contributed by syntaxin 1a and SNAP-25, and one arginine residue (R), contributed by synaptobrevin 2 (3). Sequence comparison showed that layer residues, in particular of the 0-layer, are highly conserved across the SNARE family. According to the distribution of the 0-layer residues, SNARE proteins were therefore classified into Q- and R-SNAREs (9). In addition, the presence of other asymmetric layers allowed assigning each helix to a different subfamily. Accordingly, the helices of syntaxin and of the NH_2- and COOH-terminal halves of SNAP-25 were named Qa, Qb, and Qc helix, respectively (10).

SNARE proteins are highly conserved, suggesting that they all form similar four-helix bundle structures. A proof of the principle was accomplished when the crystal structure of the late endosomal SNARE complex revealed an almost identical four-helix bundle (11). The endosomal complex consists of four independent proteins, which are relatively distant homologues of the neuronal counterparts, each contributing one helix to the bundle.

* The costs of publication of this article were defrayed in part by the payment of page charges. This article must therefore be hereby marked "*advertisement*" in accordance with 18 U.S.C. Section 1734 solely to indicate this fact.

♦ This article was selected as a Paper of the Week.

The atomic coordinates and structure factors (code 1URQ) have been deposited in the Protein Data Bank, Research Collaboratory for Structural Bioinformatics, Rutgers University, New Brunswick, NJ (http://www.rcsb.org/).

[S] The on-line version of this article (available at http://www.jbc.org) contains supplemental data (supplemental sequence identifiers for each WD repeat region).

¶ Present address: Universita' di Pavia, Dipartimento di Genetica e Microbiologia, via Abbiategrasso 207, Pavia, Italy.

‖ To whom correspondence should be addressed. Tel.: 49-551-201-1658; Fax: 49-551-201-1499; E-mail: dfassha@gwdg.de.

[1] The abbreviations used are: SNARE, SNAP receptor; SNAP, soluble *N*-ethylmaleimide-sensitive factor (NSF) attachment protein; SNAP-25, synaptosomal associated protein of 25 kDa; Cpx, complexin; Syb, synaptobrevin, Syx, syntaxin, FRET, fluorescence resonance energy transfer; OG, Oregon Green; TR, Texas Red; Lgl, lethal(2)giant larvae; MES, 4-morpholineethanesulfonic acid; PBS, phosphate-buffered saline; r.m.s.d., root mean square deviation.

Since SNARE assembly between membranes is a key reaction during synaptic secretion, many other factors regulate SNARE function. A candidate regulatory protein is tomosyn, a soluble protein of 130 kDa. Initially, tomosyn was discovered as a syntaxin 1a-binding protein, but it was also found in a larger complex together with syntaxin 1a, SNAP-25, and the putative Ca^{2+} sensor synaptotagmin (12). In addition, experiments suggested that tomosyn is capable of releasing syntaxin from its high-affinity interaction with munc18 (12), which is an essential factor for synaptic exocytosis. *In vitro* experiments imply that binding of munc18 to syntaxin 1a prevents syntaxin 1a from forming a SNARE complex with synaptobrevin 2 and SNAP-25 (13). Nevertheless, the molecular action of munc18 *in vivo* is still heavily debated (4). It was therefore suggested that tomosyn, which itself cannot support vesicle fusion because it does not possess a transmembrane region, might activate syntaxin for the formation of the fusion-active SNARE complex with synaptobrevin. However, later it was recognized that tomosyn contains a synaptobrevin-like R-SNARE motif at its very COOH terminus that allows tomosyn to form a stable complex with syntaxin 1a and SNAP-25 (14, 9). This ternary complex exhibits biophysical properties similar to the synaptic SNARE complex containing synaptobrevin (15). This suggests that a similar four-helix bundle is formed in which the R-SNARE motif of tomosyn takes over the position of synaptobrevin, but does binding of the tomosyn SNARE motif establish a four-helix bundle that is tightly structured over the entire sequence? If it indeed forms a complex similar to the synaptobrevin-containing SNARE complex, it is then structurally rather difficult to envision how tomosyn might be able to transfer syntaxin to its partner SNAREs. In that case, the SNARE motif of tomosyn might be better suited to act as a competitive inhibitor of synaptobrevin as suggested by overexpression studies (15, 16).

The COOH-terminal SNARE motif domain of tomosyn comprises only a small portion, less than 10 kDa, of a large protein. Not much is known about the function and structure of the large NH_2-terminal part of tomosyn. This region contains several WD repeats (also known as Trp-Asp or WD40 repeat). WD repeats are stretches of about 40 amino acids that typically end in Trp-Asp but exhibit only limited sequence conservation. They are typically found as several tandemly repeated units. Such repetitive segments have been shown to exist in a number of proteins, where they form the blades of a β-propeller structure; most prominent among them is β-transducin. It is now accepted that this structure serves as a binding site for other proteins.

Tomosyn is homologous to the *Drosophila* tumor suppressor protein lethal(2)giant larvae (Lgl), a WD repeat protein involved in the establishment of epithelial cell polarity during development (for reviews, see Refs. 17–19). Lgl homologs have also been discovered in yeast (Sro7p, Sro77p) (20, 21) and mammals (22). In contrast to tomosyn, Lgl homologs appear to lack a COOH-terminal SNARE motif. Nevertheless Sro7p, Sro77p, and mammalian Lgl are able to directly interact with the SNARE machinery (21, 22). It was therefore speculated that proteins of the tomosyn family are derivatives of the Lgl protein family that acquired a COOH-terminal SNARE motif during evolution (15).

Here, we present insights into the structure of the tomosyn core SNARE complex and its possible role in exocytosis

MATERIALS AND METHODS

Protein Constructs—All recombinant protein fragments were derived from cDNAs encoding for rat proteins and subcloned into the pET28a vector (Novagen), which encodes for thrombin-cleavable amino-terminal His_6-tags. The following expression constructs have been described before (23–27): a cysteine-free variant of SNAP-25A (SNAP-25, residues 1–206), a variant containing a single cysteine at position 200 (SNAP-25^{200}), the first helix (Sn1, residues 1–83), and the second helix of SNAP-25a (Sn2, residues 120–206); the soluble domain of synaptobrevin 2 (Syb, residues 1–96) and a similar fragment containing a single cysteine at position 61 (Syb^{61}); the SNARE complex forming domain of syntaxin 1a (SyxH3, residues 180–262); complexin 1 (Cpx, residues 1–134) and a complexin 1 containing a single cysteine at position 39 (Cpx^{39}).

For crystallization, shortened versions of the neuronal SNARE fragments (introduced above) were generated: the SNARE complex-forming domain of syntaxin 1A (SyxH3, residues 188–259), the first helix of SNAP-25A (Sn1, residues 7–83), the second helix of SNAP-25A (Sn2, residues 142–204), and the R-SNARE helix of synaptobrevin 2 (residues 30–89). Likewise, a shortened fragment of the SNARE complex-forming domain of tomosyn was constructed (residues 1050–1108, numbering according to the m-splice variant of tomosyn). Due to an erroneous DNA primer a frameshift at the very COOH terminus of the tomosyn fragment occurred, which added 32 amino acids of vector-derived sequence. However, this was only detected after crystallization of the tomosyn SNARE complex. These residues were probably unstructured in the tomosyn SNARE complex and were not detected in the crystal structure. For the spectroscopic investigations a slightly longer tomosyn fragment (residues 1051–1116) was used. Note that the SNAP-25 fragments present in the tomosyn SNARE complex were derived from the SNAP-25 spliceform A (P13795-2). They were also used for determine the structure of the synaptobrevin-containing SNARE complex but had been erroneously labeled as spliceform B (3, 28).

Protein Expression and Purification—All proteins were expressed in the *Escherichia coli* strain BL21 (DE3) and initially purified by Ni^{2+}-nitrilotriacetic acid affinity chromatography. After elution, His_6-tags were removed using thrombin during overnight dialysis into standard buffer (20 mM Tris, pH 7.4, 1 mM EDTA, 1 mM dithiothreitol) containing 50 mM NaCl. Proteins were further purified by ion exchange chromatography using a Mono Q or Mono S column on a Δkta system (Amersham Biosciences) essentially as described previously (23–27). The tomosyn SNARE fragment bound strongly to the Ni^{2+}-nitrilotriacetic acid matrix and was eluted using 100 mM EDTA, pH 7.4, in the presence of 5 M urea. Furthermore, as it did not bind to a Mono Q or Mono S column, it was run through both the columns. The flow-through was collected, and it contained a relatively pure tomosyn SNARE fragment. All SNARE complexes were purified using a Mono Q column after overnight assembly of the purified monomers at 4 °C. The synaptobrevin-containing core SNARE complex consisted of Syb (residues 1–96), SyxH3 (residues 180–262), Sn1 (residues 1–83), and Sn2 (residues 120–206) (23). The tomosyn SNARE complex contained the tomosyn SNARE helix, SyxH3 (residues 188–259), Sn1 (residues 7–83), and Sn2 (residues 142–204). The tomosyn SNARE complex was further purified using size exclusion chromatography on a Superdex 200 HR-10/30 column (Amersham Biosciences).

Crystallization and Data Collection—Crystals of the tomosyn SNARE complex were obtained at 20 °C by the vapor diffusion technique with hanging drops. The initial protein concentration was ≈6.5 mg/ml in standard buffer containing 100 mM NaCl. 1 μl of protein solution was mixed with 1 μl of well solution consisting of 30% (±)-2-methyl-2,4-pentanediol, 50 mM $CaCl_2$, and 50 mM MES, pH 6.0. The crystals grew as clustered, thin plates. In 2 days, after the streak seeding of preequilibrated hanging drops single, thicker plates with an average size of 0.1 × 0.4 × 0.7 mm^3 appeared. They reached their maximal size after 5 days. For data collection crystals were flashed-cooled in liquid nitrogen. Diffraction data to 2.0-Å resolution were collected at 100 K at the European Molecular Biology Laboratory BW7A synchrotron beam-line (Deutsche Electronen Synchrotron, Hamburg, Germany), using a marccd image plate scanner. Data were integrated with DENZO and scaled with SCALEPACK (29). The Collaborative Computational Program Number 4 suite of programs (30) was employed by means of its graphical interface (31) to convert the intensities to structure factor amplitudes and for subsequent calculations.

Structure Determination and Refinement—The structure of the tomosyn SNARE complex was solved by molecular replacement with AMORE (32), using the structure of the truncated synaptic core SNARE complex (28) as a search model. Automatic model building using ARP/wARP (35) alternating with Refmac refinement was performed to obtain an initial model. Further refinement consisted of iterative cycles of interactive model building by XtalView (33) and restrained refinement by minimization of a maximum likelihood function by REFMAC (34) coupled with automatic solvent building by ARP/wARP (35). Refinement and map calculation were performed with 95% of the data; 5% of randomly chosen reflections were used for the calculation of R_{free}. Fig.

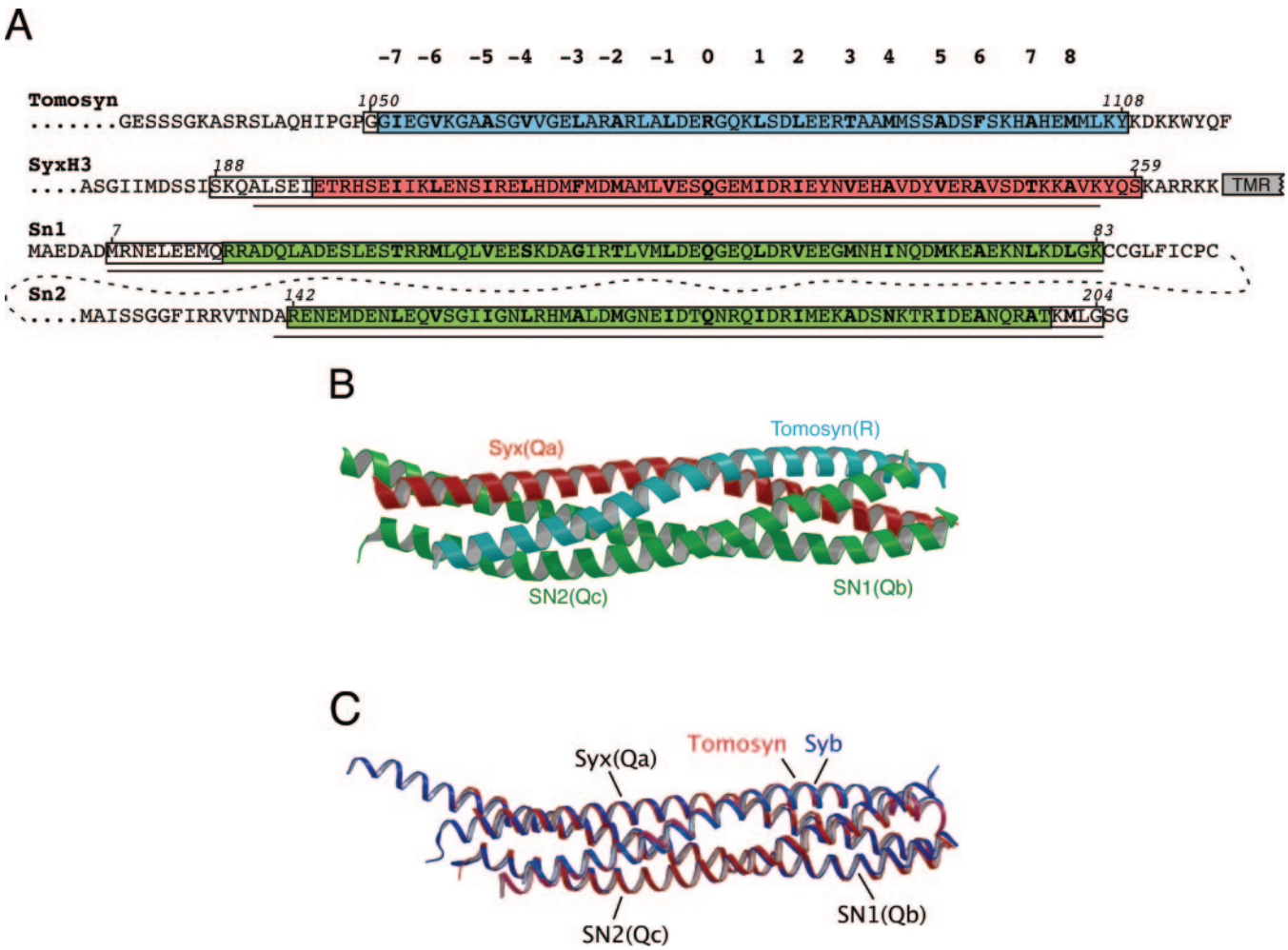

FIG. 1. **Structure of the tomosyn SNARE complex.** *A*, schematic depiction of the sequences used for crystallization. The sequences of the proteins are aligned according to the structure of the tomosyn SNARE complex. The positions of heptad repeat layers (−7 to +8) are indicated. The sequence of the constructs used for crystallization is *boxed*. The residues in the tomosyn SNARE structure are *highlighted* (tomosyn in *blue*, syntaxin in *red*, and the two SNAP-25 helices in *green*). A *dashed line* indicates the linker region between the two SNARE motifs of SNAP-25 that was not present in the tomosyn complex. The Swiss-Prot accession numbers of the proteins present in the tomosyn SNARE complex are: P32851 (syntaxin 1A), Q9Z152 (m-tomosyn), P13795-2 (SNAP-25A). *B*, schematic view of the tomosyn SNARE complex (tomosyn in *sky blue*, syntaxin in *red*, and the two SNAP-25 helices in *green*). *C*, Cα superposition of the tomosyn SNARE complex (*red*) and the synaptic SNARE complex (*blue*) (Protein Data Bank code 1N7S (28)).

1, *B* and *C*, Fig. 2, and Fig. 5*A* were prepared with MOLSCRIPT (36), BOBSCRIPT (37), and RASTER3D (38).

Fluorescence Measurements—Proteins containing a single cysteine were labeled using the sulfhydryl-reactive fluorophores Oregon Green 488 iodoacetamide or Texas Red C5 bromoacetamide. Initially, proteins were dialyzed against degassed PBS buffer (20 mM sodium phosphate, pH 7.4, 100 mM NaCl). About a 10-fold excess of the fluorescence probe was added and incubated for 2 h. The reaction was stopped by the addition of 10 mM dithiothreitol. After 1 h, the excess dye was removed by gel filtration on a Sephadex G-50 column. Afterward, the labeled protein was dialyzed against PBS buffer. Experiments were carried out in a Fluoromax-2 spectrometer equipped with autopolarizers (Jobin Yvon). All measurements were performed at 25 °C in quartz cuvettes with 1-cm path length (Hellma) using PBS buffer.

For fluorescence resonance energy transfer (FRET) measurements SNARE complexes containing labeled SNAP-25 were formed; SNAP-25^{200TR} was incubated for 2 h with SyxH3 and either Syb or tomosyn. The fluorescence spectrum using an excitation wavelength of 488 nm was recorded after complex formation. To each of the two SNARE complexes ≈300 nM Cpx^{39OG} was added, and after 5 min the spectrum was recorded again. In the crystal structure the molecular distance of the Cα-atoms of $SNAP\text{-}25^{200}$ and Cpx^{39} is about 15.4 Å (39). No change in fluorescence was observed when Cpx^{39OG} was mixed with a SNARE complex containing unlabeled Syb.

The change in the fluorescence anisotropy of Texas Red-labeled synaptobrevin (Syb^{61TR}) was measured using excitation and emission wavelengths of 590 and 610 nm, respectively. The slit widths were 2.5 and 3 nm, respectively. Initially, *G*-factor was determined according to $G = I_{HV}/I_{HH}$, where *I* is the fluorescence intensity, and the first subscript letter indicates the direction of the exciting light, and the second subscript letter is the direction of emitted light. Then the intensities of the vertically and horizontally polarized emission light after excitation by vertically polarized light were measured. The anisotropy (*r*) was calculated according to $r = (I_{VV} - G \times I_{VH})/(I_{VV} + 2 \times G \times I_{VH})$.

CD Spectroscopy—The measurements were carried out on a Jasco model J-720 instrument using quartz cuvettes with 1-cm path length (Hellma). Proteins were mixed at a concentration of 1 μM each in PBS buffer. The reaction was started by the addition of SNAP-25 to a non-interacting mix of SyxH3 with either Syb or tomosyn. For CD experiments the tomosyn helix (residues 1051–1116) was used. In addition, a shorter Syb fragment (residues 30–89) was used that corresponded to the length of the tomosyn fragment. Complex formation was followed by the change in the CD signal at 222 nm.

Sequence Analysis—New homologs of tomosyn were searched for using the Blast search tool (www.ncbi.nlm.nih.gov/blast/). In addition to the sequences used for the alignments in Fig. 6 and the supplemental data, three other tomosyn orthologs were found from the following species: *Gibberella zeae*, gi 42546760; *Candida albicans*, gi 46433698; *Eremothecium gossypii*, gi 45185876. Furthermore, we noted that the two new tomosyn homologs from *Arabidopsis thalania* had already been listed as tomosyn-like at www.tc.umn.edu/~sande099/atsnare.htm.

Initial alignments of the NH_2-terminal region of the tomosyn and Lgl proteins were performed with ClustalW (www.ebi.ac.uk/clustalw) (40). WD repeats were recognized with the help of SMART (smart.embl.de/)

TABLE I
Summary of data collection and refinement statistics

Data collection	
Space group	C2
Unit cell dimensions	a = 126.1 Å, b = 35.6 Å, c = 93.5 Å, α = 90°, β = 132.4°, γ = 90°
Resolution range/outer shell (Å)	19.39–2.00/2.03–2.00
Completeness overall/outer shell (%)	99.5/97.1
Redundancy overall/outer shell	3.5/3.4
R_{merge} overall/outer shell	0.051/0.145
Mean I/σ overall/outer shell	19/6.4
Refinement	
Reflections unique/free	19,950/1077
R_{factor}/R_{free} (%)	16.71/22.5
No. residues/water molecules	252/278
Ramachandran plot (%)	
Most favored	99.6
Additionally allowed	0.0
Generously allowed	0.4
Disallowed	0.0
r.m.s.d. bond distance (Å)	0.014
r.m.s.d. bond angle (°)	1.2
Protein average B-factor (Å^2) (A/B/C/D)	24.3/27.8/31.3/29.8
Water average B-factor (Å^2)	46.6

(41, 42) and a program on the server of the Biomolecular Engineering Research Center at Boston University (bmerc-www.bu.edu/wdrepeat/).

Other Methods—SDS-PAGE was carried out using standard procedures, except that the samples were not heated to 95 °C before analysis on the polyacrylamide gel. Non-denaturing gels were prepared and run as described previously (2). Gels were stained with Coomassie Blue.

RESULTS

Tomosyn SNARE Complex Structure—We purified a complex consisting of the SNARE motif of syntaxin 1A (SyxH3, residues 188–259), the NH_2- and COOH-terminal fragments of SNAP-25 (Sn1, residue 7–83 and Sn2, residues 141–204), and the synaptobrevin-like (R) SNARE-motif of tomosyn (residues 1050–1108, Fig. 1*A*). Crystals of the tomosyn SNARE complex grew under conditions similar to those reported for the core synaptic SNARE complex (3) and a truncated version of this complex (28). The crystals diffracted to 2.0-Å resolution and belong to space group C2. The structure of the tomosyn SNARE complex was solved by molecular replacement using the truncated synaptobrevin SNARE complex (Syb SNARE complex) (28) as a search model and refined to an R-value of 16.65% (Table I). The final model contains residues 1051–1108 of tomosyn, residues 196–259 of syntaxin, residues 16–83 of Sn1, and residues 142–200 of Sn2. In total, the model contained 252 amino acids and 278 water molecules. Statistics on data collection and refinement are reported in Table I.

The overall structure of the tomosyn SNARE complex shows an elongated, parallel four-helix bundle similar to the Syb SNARE complex (Fig. 1*B*). A superposition of its Cα atoms on those of the Syb SNARE complex is shown in Fig. 1*C*. The r.m.s.d. obtained by superposition of the identical chains, *i.e.* syntaxin residues 200–256, Sn1 residues 27–80, and Sn2 residues 147–199 (in total 164 Cα atoms), was only 0.993 Å. No significant change was observed when the tomosyn chain was included (r.m.s.d. of 1.059 Å; 222 Cα atoms). Thus, the two complexes are structurally very similar despite the fact that one of the subunits has been exchanged. The tomosyn chain occupies the same position as synaptobrevin without causing major conformational rearrangement in the other three subunits.

Superposition of the central ionic layers (Fig. 2*A*) shows only small differences in the orientation of the side chains. The r.m.s.d. is only 0.234 Å for Cα and 0.294 Å for all atoms. Most of the other layer residues were similar as well. However, in a few layers differences were observed. In layer −5 tomosyn

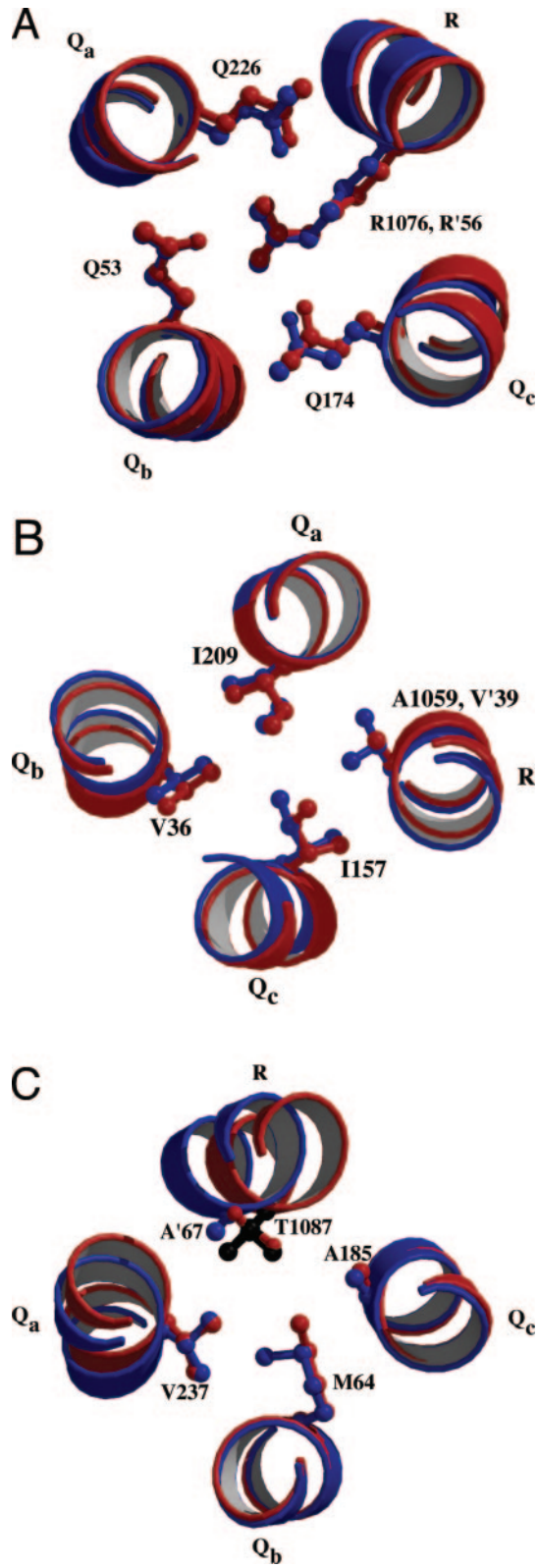

FIG. 2. **Layers.** Superposition of the heptad repeat layers 0 (*A*), −5 (*B*), and 3 (*C*) of the tomosyn SNARE complex (*red*) with the corresponding layers of the synaptic SNARE complex (*blue*). Side chains participating in layer interaction are shown as *sticks*. In *C* the side chain carbons of Thr^{1087} are shown in *black*, the oxygen is shown in *red*.

Ala^{1059} is located at the homologous position of Syb Val^{39} (Fig. 2B). Given the larger available space, SyxH3 Ile^{157} assumes another conformation, which would be sterically unfavorable in the respective layer of the Syb SNARE complex. The other

residues of this layer, however, exhibit the same orientation in the two complexes. In layer 3 of the tomosyn SNARE complex the tomosyn Thr^{1087} side chain is found in two stable conformations (Fig. 2*C*), which are stabilized through hydrogen bonds to the backbone carbonyls of Leu^{1083} and Glu^{1084}. This results in an increase of the available hydrophobic surface of Thr^{1123}, enabling a reorientation of the side chain methyl group of Sn1 Met^{64} toward the side chain of Thr^{1087}. Altogether the hydrophobic contacts in layer 3 of the tomosyn SNARE complex are strengthened, compared with the synaptic SNARE complex. Furthermore, tomosyn, similar to synaptobrevin in the synaptic complex, is anchored by a comparable number of hydrogen bonds to syntaxin and to the two SNAP-25 helices. However, the intersubunit salt bridges are differently distributed. While synaptobrevin is anchored by four salt bridges to syntaxin and by three salt bridges to Sn2, tomosyn forms only one salt bridge to syntaxin, while four salt bridges to Sn2 connect it. This difference is even stronger for the intramolecular salt bridges. While six salt bridges stabilize the synaptobrevin helix, there are 17 salt bridges along the tomosyn helix.

No Replacement—As outlined above, the substitution of synaptobrevin for the tomosyn helix did not significantly change the overall structure of the SNARE four-helix bundle. In line with these observations are the almost identical stabilities of both SNARE complexes as assessed by CD spectroscopy (15). Thus, the tomosyn SNARE complex appears to represent the final product of an assembly pathway in which the R-SNARE motif of tomosyn took over the role of synaptobrevin. However, as outlined in the introduction, tomosyn cannot act as a membrane fusion R-SNARE as it lacks a membrane anchor.

In principle, it seems possible, although unlikely, that under certain physiological conditions tomosyn simply acts as a surrogate for synaptobrevin binding. To test whether the tomosyn helix could be replaced by synaptobrevin, we made use of the "SDS resistance" of the Syb SNARE complex, *i.e.* the complex is stable in SDS sample buffer, unless heated, and migrates as one band. In contrast, the tomosyn SNARE complex did not exhibit such SDS resistance (Fig. 3*A*). Addition of tomosyn to the preformed synaptic core complex did not let the complex lose its SDS resistance. Similarly when synaptobrevin was added to the preformed tomosyn SNARE complex, no SDS-resistant complex was formed even after prolonged incubations, suggesting that synaptobrevin was not able to replace the tomosyn helix and vice versa.

As a different approach, we measured the change of fluorescence anisotropy of synaptobrevin labeled at position 61 with Texas Red (Syb^{61TR}). When Syb^{61TR} was mixed with SyxH3 and SNAP-25, a rise in fluorescence anisotropy indicative of ternary complex formation occurred (Fig. 3*B*). In contrast, mixing of Syb^{61TR} with the assembled tomosyn SNARE complex did not produce a change in the fluorescence anisotropy. Likewise, when a Syb^{61TR}-containing SNARE complex was preformed, neither addition of synaptobrevin (data not shown) nor tomosyn brought about a change in the fluorescence anisotropy. Together, this suggests that an (entire) R-SNARE helix cannot be displaced by another R-SNARE helix from an assembled SNARE complex.

Rate of Tomosyn SNARE Complex Formation—The almost identical four-helix bundle structures of the tomosyn and the Syb SNARE complex suggest that the R-SNARE motifs of tomosyn and synaptobrevin exploit the same assembly pathway. The formation of the Syb SNARE complex involves a transient 1:1 syntaxin/SNAP-25 intermediate (43, 44). Due to competition between synaptobrevin and a second syntaxin molecule for the same 1:1 intermediate, the exact rate of R-SNARE binding to this intermediate is not known yet. Nevertheless,

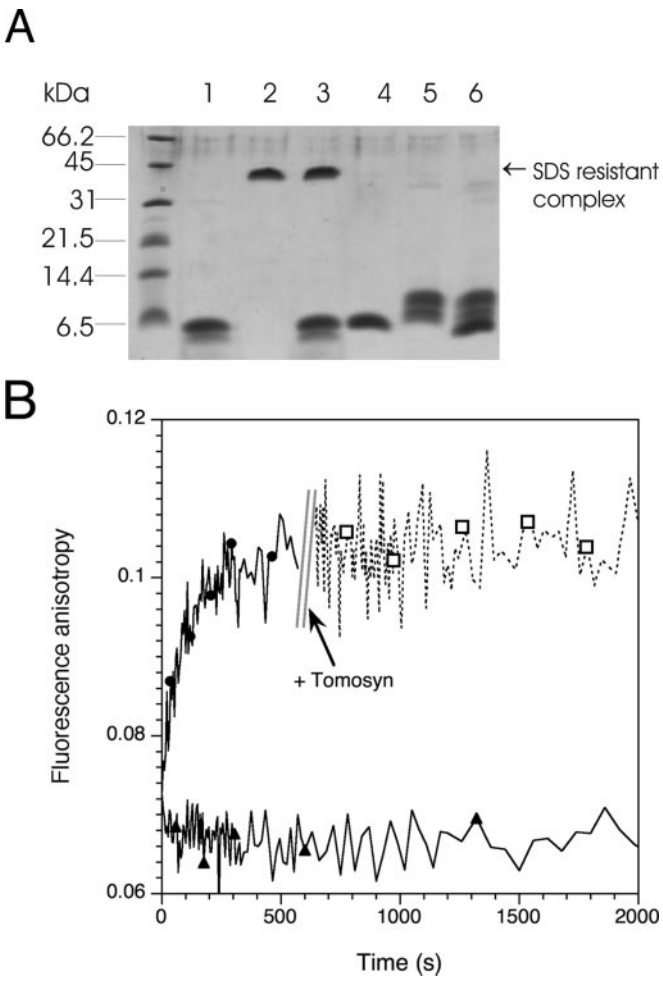

FIG. 3. **The R-SNARE helix cannot be displaced.** *A*, the synaptobrevin-containing SNARE complex runs as a single "SDS-resistant" band upon SDS-PAGE (*lane 2*). In contrast, the tomosyn-containing SNARE complex is not SDS-resistant and separates into monomers upon SDS-PAGE (*lane 5*). Addition of tomosyn to a preformed Syb SNARE complex (*lane 3*) did not, even after over night incubation, result in the disappearance of an SDS-resistant band, indicating that tomosyn did not replace the synaptobrevin helix from the complex. Similarly addition of synaptobrevin to the tomosyn SNARE complex (*lane 6*) did not result in the appearance of a SDS-resistant band, indicating that synaptobrevin did not replace the tomosyn helix from the complex. In *lane 4* individual synaptobrevin was run, and in *lane 1* the tomosyn SNARE motif was run. *B*, the formation of the ternary synaptobrevin-containing SNARE complex was followed by fluorescence anisotropy. Upon mixing of SNAP-25 and SyxH3 (2 μM, each) with synaptobrevin labeled at position 61 with Texas Red (Syb^{61TR}, ≈250 nM), a clear increase in anisotropy was observed (●), whereas when the preformed tomosyn SNARE complex (1 μM) was mixed with Syb^{61TR} no change occurred (▲). Likewise, no change in anisotropy was observed when the tomosyn SNARE motif was added, as indicated by an *arrow*, to the preformed SNARE complex containing Syb^{61TR} (□).

when we followed the formation of the synaptobrevin and of the tomosyn-containing SNARE complexes using CD spectroscopy, no significant differences in the assembly rates were observed (Fig. 4).

This suggests that both R-SNARE helices are similar in their ability to interact with syntaxin and SNAP-25.

Complexin Binding—Sequence alignment between synaptobrevin and tomosyn shows that most differences occur in residues pointing to the outside of the four-helix bundle (Fig. 5*A*). Accordingly, it might be possible that the assembled tomosyn SNARE complex recruits factors to its surface, which are different from Syb SNARE complex. For example, the soluble protein complexin has been shown to specifically form a high-

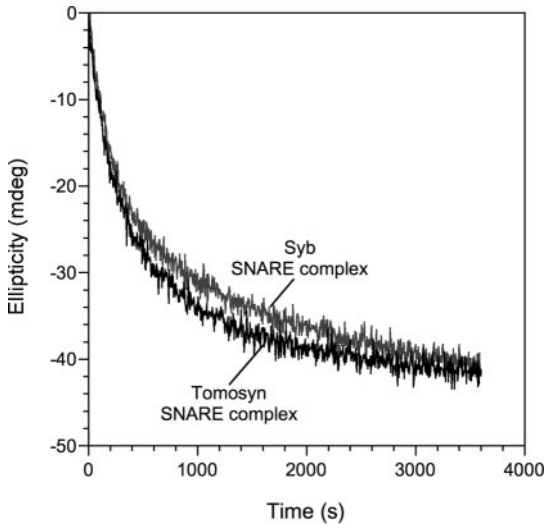

FIG. 4. **The synaptobrevin and the tomosyn SNARE complex form with similar rates.** Since the formation of SNARE complexes is accompanied by major structural changes, we measured the change of the CD signal at 222 nm to compare the rates of the assembly of the synaptobrevin- (*gray*) and the tomosyn-containing SNARE complex (*black*). The rates of SNARE complex formation were not significantly different.

affinity complex with the synaptobrevin-containing SNARE complex (26, 27, 39, 45). The central helical region of complexin binds in an antiparallel orientation to the groove formed by the synaptobrevin and syntaxin helices. A structural comparison of the complexin interacting region of synaptobrevin with the homologous region of tomosyn (Fig. 5*A*) suggested that the tomosyn SNARE complex might not be able to undergo strong interactions with complexin. In detail, Cpx Arg^{48} forms salt brigdes with Syb Asp^{68} and Syb Asp^{65}, and the two Cpx residues Arg^{59} and Arg^{63} form salt brigdes with Syb Asp^{57}. In addition, a hydrogen bond exists between Cpx Tyr^{52} and Syb Asp^{64}. Furthermore, at the COOH-terminal end of the complexin/synaptobrevin interface, a hydrophobic pocket is formed between Cpx Met^{62}, Cpx Ile^{66}, Syb Leu^{54}, and Syb Val^{50} (39). Most of these interactions cannot be formed when Syb is replaced by tomosyn.

The association between complexin and the synaptic SNARE complex is sufficiently stable to visualize it as a single band in nondenaturing PAGE. When we tested the interaction between complexin with the tomosyn complex, however, no such tight association was detected (Fig. 5*B*). The interaction between complexin and SNARE complexes containing synaptobrevin or tomosyn was also tested using FRET. In contrast to non-denaturing PAGE, this approach allowed us to follow the interaction in equilibrium. Complexin, labeled with Oregon Green (Cpx^{39OG}), was used as the fluorescence donor. SNAP-25, labeled with Texas Red at the COOH-terminal end of the second SNARE helix ($SNAP\text{-}25^{200TR}$), was used as the fluorescence acceptor. With $SNAP\text{-}25^{200TR}$ a SNARE complex containing either synaptobrevin or tomosyn was formed. When Cpx^{39OG} was mixed with the Syb SNARE complex, pronounced quenching of the donor fluorescence, indicative of FRET, was observed, but no quenching was detectable upon mixing of Cpx^{39OG} with the tomosyn SNARE complex (Fig. 5*C*).

Evolutionary Conservation of Tomosyn—Originally, tomosyn has been suggested to act as an essential part of synaptic release machinery. Yet, at least one of the three splice variants of rat tomosyn, b-tomosyn, is ubiquitously expressed, hinting at a broader function of tomosyn in vesicular trafficking. Our data bank searches revealed several new homologs of tomosyn. Most astonishingly we found true tomosyn homologs among the Plantae and Fungi kingdoms (see Fig. 6 legend for details). All tomosyn homologs possess conserved WD repeats in the NH_2-terminal half (supplemental data) and an R-SNARE motif at the very COOH terminus (Fig. 6). The SNARE motif in Metazoa, Plantae, and several Fungi is well preserved. Yet, the SNARE motif of some fungal tomosyns appears to be mainly conserved in the layers COOH-terminal to the 0-layer arginine. Since we did not discover an obvious tomosyn homolog in the yeast *S. cerevisiae*, we reexamined the sequence of the proteins Sro7p and Sro77p. These two proteins had been reported not to contain a SNARE motif and were therefore classified as Lgl protein homologs (20, 21). However, both proteins are highly homologous to the newly discovered Fungi tomosyns in a region directly upstream of the putative SNARE motif (data not shown). A closer inspection of the putative SNARE motif region revealed an arginine residue in Sro7p (Arg^{979}) and in Sro77p (Arg^{956}), which might be able to serve as the 0-layer position of an R-SNARE motif. However, in a ClustalW alignment (not shown here) the leucine of the following heptad repeat (Leu^{986} in Sro7p and Leu^{963} in Sro77p) was aligned with the 0-layer arginine of other Fungi tomosyns. No obvious continuation of the heptad motif upstream of the putative 0-layer arginine of Sro7p and Sro77p was found. Possibly, this indicates a tendency for a partial loss of the COOH-terminal R-SNARE motif in some Fungi subdivisions. A similar tendency might be evident in a second tomosyn-like protein in *A. thalania* (tom2-*AT*), which exhibits an asparagine in the 0-layer position. It also possesses a glutamate in the putative −4 layer. A similar feature was seen in the endosomal SNARE complex, which accommodates a charged residue (Glu^{200} of syntaxin 8) in layer 6 without interrupting the coiled-coil periodicity (11). Taken together, the presence of tomosyn-like proteins that possess a large NH_2-terminal WD repeat-rich region and a COOH-terminal R-SNARE-like motif through all eukaryotic divisions implies a conserved function of these proteins.

DISCUSSION

The soluble protein tomosyn possesses a synaptobrevin-like SNARE motif at its very COOH-terminal end. Tomosyn was found complexed with the plasma membrane SNAREs syntaxin 1 and SNAP-25. This complex was suggested to resemble the synaptobrevin 2-containing SNARE complex. The lack of a membrane anchor, however, does not allow tomosyn to act as a true, fusion-active synaptobrevin during synaptic exocytosis. Here, we show the crystal structure of the core SNARE complex containing the SNARE helices of syntaxin 1a, SNAP-25a, and tomosyn. It comprises a four-helix bundle structure almost identical to the Syb SNARE complex (3, 28). This structural similarity makes it rather difficult to envision that tomosyn acts as an essential part of a cascade of protein-protein interactions that ultimately lead to the formation of the membrane-bridging trans-SNARE complex. The tomosyn and the Syb SNARE complexes are highly stable and exhibit a marked hysteresis in the folding-unfolding transitions (15, 43). In addition, we found that the tomosyn SNARE motif cannot be replaced from this stable assembly by synaptobrevin and vice versa. Together this indicates that both complexes represent final products and require the ATPase *N*-ethylmaleimide-sensitive factor for disassembly and reuse. Furthermore, we did not find a significant difference in the rate with which synaptobrevin 2 and the tomosyn SNARE motif assemble into a ternary SNARE complex, indicating that tomosyn uses the same assembly pathway as synaptobrevin 2. Similar results were obtained when endobrevin, another distant homologue of synaptobrevin 2, was used (data not shown), suggesting that different R-SNAREs can interact with similar efficiency with a transient intermediate of the Q-SNAREs syntaxin 1a and

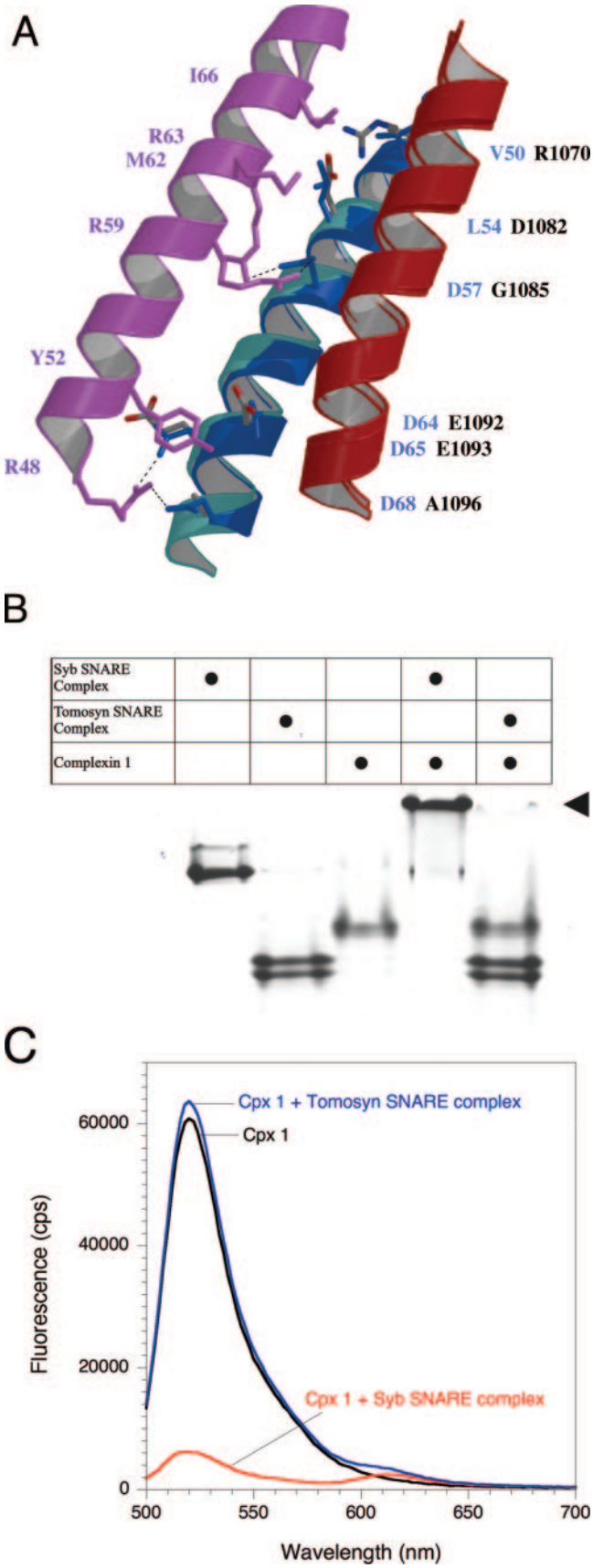

FIG. 5. **Complexin does not bind to the tomosyn SNARE complex.** *A*, ribbon diagram of complexin 1 (Cpx) bound to the surface of the neuronal SNARE complex. Cpx (*pink*) interacts with residues along the groove between the Syb (*blue*) and Syx (*red*) helices. For simplification, both SNAP-25 helices are omitted. For structural comparison, Syb was overlaid with tomosyn (*sky blue*) of the tomosyn SNARE complex. Side chains are shown as *sticks* in the same color code as the ribbon, except for tomosyn: *gray* (carbons), *red* (oxygens), and blue (nitrogens). Salt bridges between Cpx and Syb side chains are shown as *dotted lines*. *B*, the high-affinity complex (*arrowhead*) between Cpx and the Syb SNARE complex can be separated by non-denaturing PAGE from its constituents (26). Almost no complex band was observed upon mixing of Cpx and the tomosyn SNARE complex. Note that the tomosyn SNARE complex ran as a *double band*. *C*, a ternary SNARE complex containing SNAP-25 labeled at position 200 with Texas Red, SyxH3, and either the Syb or the tomosyn SNARE complex was preformed. These preformed SNARE complexes were mixed with Cpx labeled at position 39 with Oregon Green, Cpx^{39OG}. Upon excitation at 488 nm a pronounced decrease in donor fluorescence, indicative of FRET, was observed when Cpx^{39OG} was mixed with the Syb SNARE complex (*red*) but not upon mixing with the tomosyn SNARE complex (*blue*). The spectrum of Cpx^{39OG} alone is shown in *black*.

SNAP-25 (44). This strengthens the view that R-SNARE binding is less selective, whereas the formation of the Qabc-intermediate probably contributes to SNARE specificity.

Although the exchange of the R-SNARE helix did not significantly change the overall structure and properties of the complex, it brought about several changes on the surface of the complex along the tomosyn helix. For instance these changes abolished the interaction with the protein complexin, which binds with high affinity onto the surface of the Syb SNARE complex (26, 27, 39, 45). It seems possible that tomosyn might recruit different modulating factors onto the surface of the four-helix bundle.

In the crystal structure the tomosyn helix does not show strong interactions with the neighboring syntaxin helix. However, tomosyn was originally affinity-purified using glutathione *S*-transferase-syntaxin, a result that hints at a tight interaction between the two proteins (12). In addition, although the syntaxin-binding region of tomosyn was mapped to its bare SNARE motif, only high concentrations of this tomosyn fragment inhibited binding of tomosyn to glutathione *S*-transferase-syntaxin (46). Altogether, this suggests that regions upstream of the SNARE motif of tomosyn or syntaxin might be involved in binding. On the other hand, the overexpressed NH_2-terminal region of tomosyn, *i.e.* in the absence of the SNARE motif, was not found in a stable complex with syntaxin and SNAP-25 (15).

The participation of other regions of tomosyn in binding might also be deduced from the observation that proteins of the homologous Lgl family, which exhibit similar domain architecture but do not possess an apparent SNARE motif, interact with SNARE proteins as well. For example, the yeast proteins Sro7p and Sro77p were shown to interact with the yeast SNAP-25 homolog Sec9p (21). Interestingly, our closer inspection revealed that Sro7p and Sro77p do posses a COOH-terminal heptad repeat sequence. Additionally, it indicated that this stretch, although it is somewhat rudimentary, clearly originated from an R-SNARE motif, which is intact in other Fungi tomosyn homologs (Fig. 6). The mammalian Lgl1 (Mlgl) was also shown to interact with SNARE proteins (22). Intriguingly, Lgl1 exhibits moderate coiled-coil probability at the very COOH terminus as well, although it is unclear whether this was a remnant of a former R-SNARE motif. Thus, it seems possible that the COOH-terminal stretches of Lgl1 or Sro7p/Sro77p are mainly responsible for SNARE binding. However, in these proteins the region responsible for SNARE binding still remains unknown.

Although tomosyn does not possess a membrane anchor, its coiled-coil layers advance until the point at which in "fusion-competent" R-SNAREs the membrane anchor region begins. The SNARE complex formed by tomosyn is structured until close to the membrane anchor regions. Interestingly, the very COOH terminus of tomosyn contains several aromatic and

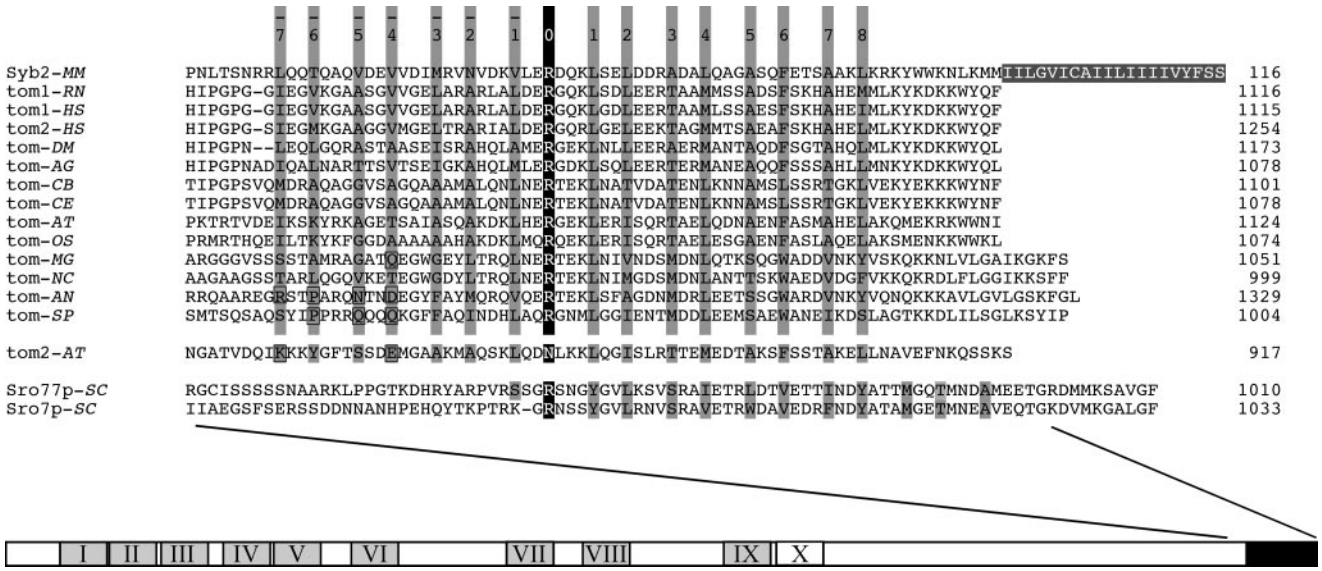

FIG. 6. **Sequence alignment of the R-SNARE motif region of tomosyn-like proteins.** The R-SNARE motif of synaptobrevin 2 (*Mus musculus:* gi 207626, Syb2-*MM*) and several tomosyn homologs from the following species were aligned: *Rattus norvegicus* (gi 13540648, tom1-*RN*); *Homo sapiens* (gi 31652247, tom1-*HS*, and gi 41146546, tom2-HS); *Caenorhabditis elegans* (gi 17508275, tom-*CE*); *Caenorhabditis briggsae* (gi 39598218, tom-*CB*); *Drosophila melanogaster* (gi 28571171, tom-*DM*); *Anopheles gambiae* (gi 31204405, tom-*AG*); *Magnaporthe grisea* (gi 38102429, tom-*MG*); *Neurospora crassa* (gi 32423373, tom-*NC*); *Aspergillus nidulans* (gi 40741778, tom-*AN*); *Schizosaccharomyces pombe* (gi 19113918, tom-*SP*); *Oryza sativa* (gi 34898238, tom-*OS*). *A. thalania* (gi 15239173, tom1-*AT*, and gi 15237037, tom2-*AT*). The transmembrane region at the COOH terminus of synaptobrevin 2 is indicated *white on gray background*. The number of the layers is indicated on the *top*. The central 0-layer containing the highly conserved arginine is indicated *white on a black background*. Other layer residues are shown in *black on a gray background*. Note that one *Arabidopsis* tomosyn (tom2-*AT*) and several Fungi tomosyn homologs have hydrophilic residues (*boxed*) in putative heptad repeat layers upstream of the 0-layer. It is unclear whether these residues can form a hydrophobic interior of a SNARE helix bundle. It is possible that a stutter or a skip can explain the apparent break in the heptad repeat periodicity of these homologs. We also aligned the COOH-terminal end of the two tomosyn-like proteins Sro7p (gi 6325289, Sro7p-*SC*) and Sro77p (gi 6319362, Sro77p-*SC*) from *Saccharomyces cerevisia* to indicate that these proteins might still possess a partial R-SNARE motif. A schematic depiction of the domain structure of tomosyn is given underneath. The COOH-terminal R-SNARE motif is shown in *black*. Putative WD repeats in the NH_2-terminal region are *boxed*.

basic residues, which might be able to penetrate into the membrane-water interface. This substantiates the view that *in vivo* the COOH-terminal end of tomosyn comes close to a membrane surface. Complete formation of the tomosyn SNARE complex would therefore inhibit the plasma membrane Q-SNAREs to receive the vesicular synaptobrevin. It has therefore been suggested that tomosyn might restrict the accessible Q-SNAREs and thus fusion sites in the plasma membrane (15). This scenario is corroborated by the finding that overexpression of tomosyn reduced the number of exocytotic events but did not changed the properties of a single of fusion event (15, 16).

Our sequence analysis suggests that the R-SNARE motif is a deep-rooted and well preserved characteristic of tomosyn-like proteins, because it is also present in tomosyn homologs from the Fungi and Plantae kingdoms. Yet the SNARE motif of tomosyn comprises less than 10% of its sequence. Not much is known about the structure and function of the remaining NH_2-terminal region. Much attention has been drawn to the homologous WD repeats in the NH_2-terminal region of tomosyn and Lgl proteins (supplemental data). However, WD repeats occur in many molecules with a variety of different functions, and therefore no function in tomosyn can be delineated from this. Nevertheless, the close homology between the Lgl and tomosyn protein families infers that they carry out related functions. For example, deletion of the two yeast proteins Sro7p and Sro77p has been shown to evoke a strong cold-sensitive block in exocytosis (21). The double mutant also shows an increased susceptibility to NaCl stress, which results from mis-sorting of the sodium extruding ATPase (47). *Drosophila* Lgl functions in a common genetic pathway with the other tumor suppressor genes Scribble and Disc large (Dlgl). These three gene products are dependent on each other for correct localization. Mutations in any of these lead to a loss of apical-basal polarity (48). It was suggested that uncontrolled growth in these mutants arises from a defect in vesicular trafficking, which in turn leads to a mislocalization of signaling molecules (for a more detailed discussion of the role of Lgl, see Refs. 17–19). An alternative view arises from the fact that Sro7p and Sro77p show strong genetic interactions with the yeast myosins Myo1p and Myo2p and act downstream of the Rho3 GTPase (20). In the same way, Lgl might regulate cell polarity through the actin cytoskeleton. For example, deletion of the Lgl1 gene in mouse leads to a drastic pertubation in the organization of the actin cytoskeleton but not to an accumulation of transport vesicles (49). Taken together, Lgl appears to be a crucial factor that is most likely involved in the regulation of vesicular trafficking in polarized cells.

A possibly analogous role was recently discovered for tomosyn: it was found to guide plasmalemmal precursor vesicles to the leading edges of growth cones in neurites by preventing the fusion of these vesicles at the palms of growth cones (50). Probably tomosyn preferentially forms SNARE complexes at the palms of growth cones, which leaves only the Q-SNARE acceptor sites at the leading edge open to engage with vesicular synaptobrevin. Interestingly, formation of the tomosyn complex is triggered through phosphorylation of syntaxin 1 by the Rho-associated serine/threonine kinase ROCK (50).

So far tomosyn has been mostly implicated in vesicular trafficking in neurosecretory cells (12, 15, 16, 50, 51). Yet, the b-tomosyn spliceform is present in other tissues as well (46) and has been shown to interact with the exocytotic Q-SNAREs syntaxin 4 and SNAP-23 (52). Our data bank searches revealed that tomosyn is present in all branches of the eukaryotic tree, pointing toward a broader function of tomosyn in membrane trafficking, most likely during regulated exocytosis. So far, Q-SNAREs are the only interacting partners of tomosyn known, a fact that hampers the integration of tomosyn into the current model of exocytosis. Nevertheless, the structure of the

core tomosyn SNARE complex clearly shows that tomosyn cannot act as a surrogate for synaptobrevin in exocytosis. On the contrary, it is more likely that tomosyn acts as a negative regulator of exocytosis by inhibiting binding of the vesicular R-SNARE to the plasma membrane Q-SNARE acceptor. Furthermore, it is tempting to speculate that the NH_2-terminal region of tomosyn, which is enriched in WD repeats, might link the SNARE complex to a signaling pathway, such as envisaged for the Lgl-like proteins involved in cell polarity. For SNAREs, such a signaling pathway may be involved in the regulation of exocytosis.

Acknowledgments—We thank Henning Urlaub and Uwe Plessmann for the mass spectrometric analyses that were done to confirm the identities of protein fragments in the complex. We thank Reinhard Jahn and Matthew Holt for fruitful discussions and critical reading of the manuscript.

REFERENCES

1. Fasshauer, D., Bruns, D., Shen, B., Jahn, R., and Brünger, A. T. (1997) *J. Biol. Chem.* **272,** 4582–4590
2. Fasshauer, D., Otto, H., Eliason, W. K., Jahn, R., and Brünger, A. T. (1997) *J. Biol. Chem.* **272,** 28036–28041
3. Sutton, R. B., Fasshauer, D., Jahn, R., and Brunger, A. T. (1998) *Nature* **395,** 347–353
4. Rizo, J., and Sudhof, T. C. (2002) *Nat. Rev. Neurosci.* **3,** 641–653
5. Rettig, J., and Neher, E. (2002) *Science* **298,** 781–785
6. Jahn, R., Lang, T., and Sudhof, T. C. (2003) *Cell* **112,** 519–533
7. Fasshauer, D. (2003) *Biochim. Biophys. Acta* **1641,** 87–97
8. Ungar, D., and Hughson, F. M. (2003) *Annu. Rev. Cell Dev. Biol.* **19,** 493–517
9. Fasshauer, D., Sutton, R. B., Brünger, A. T., and Jahn, R. (1998) *Proc. Natl. Acad. Sci. U. S. A.* **95,** 15781–15786
10. Bock, J. B., Matern, H. T., Peden, A. A., and Scheller, R. H. (2001) *Nature* **409,** 839–841
11. Antonin, W., Fasshauer, D., Becker, S., Jahn, R., and Schneider, T. R. (2002) *Nat. Struct. Biol.* **9,** 107–111
12. Fujita, Y., Shirataki, H., Sakisaka, T., Asakura, T., Ohya, T., Kotani, H., Yokoyama, S., Nishioka, H., Matsuura, Y., Mizoguchi, A., Scheller, R. H., and Takai, Y. (1998) *Neuron* **20,** 905–915
13. Yang, B., Steegmaier, M., Gonzalez, L. C., Jr., and Scheller, R. H. (2000) *J. Cell Biol.* **148,** 247–252
14. Masuda, E. S., Huang, B. C., Fisher, J. M., Luo, Y., and Scheller, R. H. (1998) *Neuron* **21,** 479–480
15. Hatsuzawa, K., Lang, T., Fasshauer, D., Bruns, D., and Jahn, R. (2003) *J. Biol. Chem.* **278,** 31159–31166
16. Yizhar, O., Matti, U., Melamed, R., Hagalili, Y., Bruns, D., Rettig, J., and Ashery, U. (2004) *Proc. Natl. Acad. Sci. U. S. A.* **101,** 2578–2583
17. Wodarz, A. (2000) *Curr. Biol.* **10,** R624–R626
18. Justice, N. J., and Jan, Y. N. (2003) *Nat. Cell Biol.* **5,** 273–274
19. Humbert, P., Russell, S., and Richardson, H. (2003) *BioEssays* **25,** 542–553
20. Kagami, M., Toh-e, A., and Matsui, Y. (1998) *Genetics* **149,** 1717–1727
21. Lehman, K., Rossi, G., Adamo, J. E., and Brennwald, P. (1999) *J. Cell Biol.* **146,** 125–140
22. Musch, A., Cohen, D., Yeaman, C., Nelson, W. J., Rodriguez-Boulan, E., and Brennwald, P. J. (2002) *Mol. Biol. Cell* **13,** 158–168
23. Fasshauer, D., Eliason, W. K., Brünger, A. T., and Jahn, R. (1998) *Biochemistry* **37,** 10354–10362
24. Fasshauer, D., Antonin, W., Margittai, M., Pabst, S., and Jahn, R. (1999) *J. Biol. Chem.* **274,** 15440–15446
25. Margittai, M., Fasshauer, D., Pabst, S., Jahn, R., and Langen, R. (2001) *J. Biol. Chem.* **276,** 13169–13177
26. Pabst, S., Hazzard, J. W., Antonin, W., Südhof, T. C., Jahn, R., Rizo, J., and Fasshauer, D. (2000) *J. Biol. Chem.* **275,** 19808–19818
27. Pabst, S., Margittai, M., Vainius, D., Langen, R., Jahn, R., and Fasshauer, D. (2002) *J. Biol. Chem.* **277,** 7838–7848
28. Ernst, J. A., and Brunger, A. T. (2003) *J. Biol. Chem.* **278,** 8630–8636
29. Otwinowski, Z., and Minor, W. (1997) *Methods Enzymol.* **276,** 307–326
30. Winn, M. D., Ashton, A. W., Briggs, P. J., Ballard, C. C., and Patel, P. (2002) *Acta Crystallogr. Sect. D Biol. Crystallogr* **58,** 1929–1936
31. Potterton, E., Briggs, P., Turkenburg, M., and Dodson, E. (2003) *Acta Crystallogr. Sect. D Biol. Crystallogr.* **59,** 1131–1137
32. Navaza, J. (2001) *Acta Crystallogr. Sect. D Biol. Crystallogr.* **57,** 1367–1372
33. McRee, D. E. (1999) *J. Struct. Biol.* **125,** 156–165
34. Murshudov, G. N., Vagin, A. A., Lebedev, A., Wilson, K. S., and Dodson, E. J. (1999) *Acta Crystallogr. Sect. D Biol. Crystallogr.* **55,** 247–255
35. Perrakis, A., Morris, R., and Lamzin, V. S. (1999) *Nat. Struct. Biol.* **6,** 458–463
36. Kraulis, P. J. (1991) *J. Appl. Crystallogr.* **24,** 946–950
37. Esnouf, R. M. (1999) *Acta Crystallogr. Sect. D Biol. Crystallogr.* **55,** 938–940
38. Merrit, E. A., and Bacon, D. J. (1997) *Methods Enzymol.* **277,** 505–524
39. Chen, X., Tomchick, D. R., Kovrigin, E., Arac, D., Machius, M., Sudhof, T. C., and Rizo, J. (2002) *Neuron* **33,** 397–409
40. Thompson, J. D., Higgins, D. G., and Gibson, T. J. (1994) *Nucleic Acids Res.* **22,** 4673–4680
41. Schultz, J., Milpetz, F., Bork, P., and Ponting, C. P. (1998) *Proc. Natl. Acad. Sci. U. S. A.* **95,** 5857–5864
42. Letunic, I., Copley, R. R., Schmidt, S., Ciccarelli, F. D., Doerks, T., Schultz, J., Ponting, C. P., and Bork, P. (2004) *Nucleic Acids Res.* **32,** D142–D144
43. Fasshauer, D., Antonin, W., Subramaniam, V., and Jahn, R. (2002) *Nat. Struct. Biol.* **9,** 144–151
44. Fasshauer, D., and Margittai, M. (2004) *J. Biol. Chem.* **279,** 7613–7621
45. Bracher, A., Kadlec, J., Betz, H., and Weissenhorn, W. (2002) *J. Biol. Chem.* **277,** 26517–26523
46. Yokoyama, S., Shirataki, H., Sakisaka, T., and Takai, Y. (1999) *Biochem. Biophys. Res. Commun.* **256,** 218–222
47. Wadskog, I., Maldener, C., Proksch, A., Madeo, F., and Adler, L. (2004) *Mol. Biol. Cell* **15,** 1436–1444
48. Bilder, D., Li, M., and Perrimon, N. (2000) *Science* **289,** 113–116
49. Klezovitch, O., Fernandez, T. E., Tapscott, S. J., and Vasioukhin, V. (2004) *Genes Dev.* **18,** 559–571
50. Sakisaka, T., Baba, T., Tanaka, S., Izumi, G., Yasumi, M., and Takai, Y. (2004) *J. Cell Biol.* **166,** 17–25
51. Kraut, R., Menon, K., and Zinn, K. (2001) *Curr. Biol.* **11,** 417–430
52. Widberg, C. H., Bryant, N. J., Girotti, M., Rea, S., and James, D. E. (2003) *J. Biol. Chem.* **278,** 35093–35101